JPE 17-3-12

https://doi.org/10.6113/JPE.2017.17.3.695
ISSN(Print): 1598-2092 / ISSN(Online): 2093-4718

An Approach for Identifying the Temperature of Inductance Motors by Estimating the Rotor Slot Harmonic Based on Model Predictive Control

Liguo Wang†, Qingyue Jiang*, Chaoyu Zhang*, Dongxin Jin*, and Hui Deng**

†,*Department of Electrical and Electronics Engineering, Harbin Institute of Technology, Harbin, China
**Daqing Oilfield Powerlift Pump Industry Co. Ltd., Daqing, China

Abstract

In order to satisfy the urgent requirements for the overheating protection of induction motors, an approach that can be used to identify motor temperature has been proposed based on the rotor slots harmonic (RSH) in this paper. One method to accomplish this is to improve the calculation efficiency of the RSH by predicting the stator winding distribution harmonic order by analyzing the harmonics spectrum. Another approach is to increase the identification accuracy of the RSH by suppressing the influence of voltage flashes or current surges during temperature estimation based on model predictive control (MPC). First, an analytical expression of the stator inductance is extracted from a steady-state positive sequence motor equivalent circuit model developed from the rotor flux field orientation. Then a procedure that applies MPC for reducing the identification error of the rotor temperature caused by voltage sag or swell of the power system is given. Due to this work, the efficiency and accuracy of the RSH have been significantly improved and validated our experiments. This work can serves as a reference for the on-line temperature monitoring and overheating protection of an induction motor.

Key words: Model predictive control (MPC), Overheating protection, Rotor slot harmonic (RSH), Sensor-less identification

I. INTRODUCTION

Like the model reference adaptive control method, when rotor slots harmonic (RSH) theory is used to identify temperature, which is difficult to measure directly, it is necessary to improve the calculation efficiency and identification accuracy of the RSH [1]-[4]. Research shows that it is of great significance to set a temperature protection limit and to increase the response speed of overheating failure protection for an induction motor [5], [6]. As a matter of fact, there are many factors that affect the accuracy and efficiency of the identification of temperature, such as the uncertainty of the harmonic order, the complexity of the motor parameters, and most of all, the stator voltage transient shock [7]-[11]. These reasons serve as a motivation to find an effective way of modelling a motor and forecasting its parameters in order to determine upper temperature protection limit online by obtaining the motor temperature rapidly and accurately.

MPC has being successfully used in the parameter estimation and prediction of induction motors, fault protection of wind power generators, and trajectory control of robot motion. MPC is more appropriate for calculating future control actions by solving at each sampling time an optimization problem specified over a certain prediction horizon for a given system model [12]-[15]. The main drawback of the RSH is that it often wastes a lot of computer-time and is greatly influenced by voltage sags or swells of power systems. Meanwhile, improvements should be made to make up for the above shortcomings of the RSH. Since MPC have great advantages in terms of predicting and correcting parameters, it is used to improve the identification accuracy of the RSH by compensating the voltage and current perturbation of the power system.

This paper is organized as follows. Section II estimates the stator winding distribution harmonic order and the corresponding slot harmonic frequency by comparing the

Manuscript received Aug. 23, 2016; accepted Jan. 31, 2017
Recommended for publication by Associate Editor Bon-Gwan Gu.
†Corresponding Author: wlg2001@hit.edu.cn
Tel: +86-451-86413050, Fax: +86-451-86413050, Harbin Inst. of Tech.
*Dept. of Electrical and Electronics Eng., Harbin Inst. of Tech., China
**Daqing Oilfield Powerlift Pump Industry Co. Ltd., China

spectrum of the stator current with the harmonics. Section III derives the analytical expressions of the motor parameters such as the stator inductance based on modelling the steady-state positive sequence motor equivalent circuit. It also gives the application procedure of MPC to correct and optimize the calculated motor parameters. Section IV validates the feasibility and effectiveness of MPC in the compensation of the identification error of the RSH. Experiments show that this work can significantly improve the accuracy of the RSH. This is demonstrated by comparing the identifying temperature with the actual measured temperature.

The main contributions of this paper include the prediction of the harmonic order, the analytical solution of the motor parameters, and the estimation and correction procedure of the MPC. This optimization approach has been employed successfully in identifying the rotor temperature of an induction motor under the condition that stator voltage suddenly changed. Due to this work the efficiency and the accuracy of the RSH has been significantly improved.

II. IMPROVEMENT OF THE RSH EFFICIENCY

Since the air gap flux is linked to the stator windings, the variations in the air gap flux are reflected in the stator current spectrum. The rotor speed can be extracted from the stator current spectrum, which is the basis of the RSH.

A. The Issue of the RSH

When the RSH is used to estimate the rotor temperature of an inductance motor both the identification accuracy and calculation efficiency should be increased. According to [1], [2], the RSH can be described by the following expression:

$$f_{sh} = f_1\left(kR(1-s)/(p/2)+n_w\right) \quad (1)$$

Where, $f_1 = 50\text{Hz}$ denotes the fundamental frequency of the positive-sequence voltage of the power supply, which is applied to the terminals of an inductance motor, R is the number of rotor slots; s is per unit slip; p is the number of poles; and $n_w = \pm1, \pm2, \pm3, \cdots$ is the harmonic order, where $k = 1, 2, \cdots$ indicates the rotor MMF (the rotor magneto-motive forces) distribution harmonic order.

For an inductance motor, since the parameters that consists of f_1, p, R and k (generally, $k = 1$) depend on the structural characteristics of the motor, which are in general unknown to the user, it is necessary to predict the harmonic order n_ω in order to increase the estimation efficiency.

Actual measured results show that the motor temperature is an inertia variable which does not mutate suddenly as the perturbation of the stator current of the inductance motor. According to the RSH, the identification temperature is related to the positive-sequence voltage and the current where transient power quality issues have been becoming extrusive, such as voltage swells and voltage sags. These reasons make the identification temperature have sudden changes which do not relate the swell with the actual motor temperature. Therefore, fluctuation in the voltage and current should be taken into account in order to raise the identification accuracy.

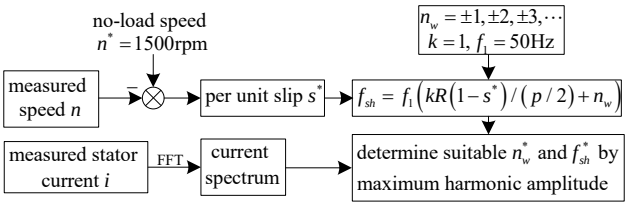

Fig. 1. Scheme of the harmonic order n_w prediction algorithm.

For the purpose to improving the efficiency and accuracy of slots harmonic extraction, it is necessary to predict a reasonable harmonic order for online temperature monitoring. The process of harmonic order pre-setting is demonstrated as follows:

1) Sample the stator current.
2) Measure rotation speed *n* and calculate the rotor slip *s*.
3) Predict the harmonic frequencies in different harmonic orders after substituting slip *s* into formula (1).
4) Extract the spectrum of the stator current using Fourier transformation and determine the harmonic order n_w.
5) Take the prediction value n_w as a desired slot harmonic order into the online speed identification algorithm.

B. Prediction of the Harmonic Order n_w

A Y90L-4 type 1.5kW inductance motor was used to demonstrate the prediction process of the harmonic order n_w. The motor parameters are as follows: $R = 22$, $p = 4$, and $k = 1$.

Fig. 1 shows the scheme of the prediction algorithm of the harmonic order n_w. First, it is possible to obtain a total of $2 \times n_w$ rotor slot harmonic frequencies f_{sh} from (1) based on the actual per unit slot s^* under the condition of $n_w = \pm1, \pm2, \pm3, \cdots$ and $k = 1$. Then it is necessary to determine suitable n_w^* and f_{sh}^* as prediction values by comparing f_{sh} with the stator current spectrum. Some of the measured and analyzed results are shown in Fig. 2 to Fig. 4.

As shown in Fig. 2, the measured rotor speed n was recorded by an independent tachometer. Fig. 3 shows the arithmetic means of sampled speed and the corresponding per unit slot s^* within 0.8s. There are total 40 fundamental periods all of them correspond to an arithmetic mean of a fundamental period.

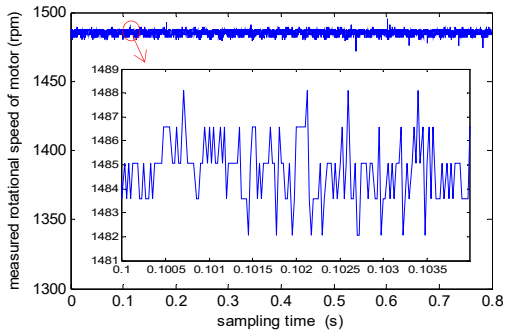

Fig. 2. Measured rotational speed obtained with a tachometer.

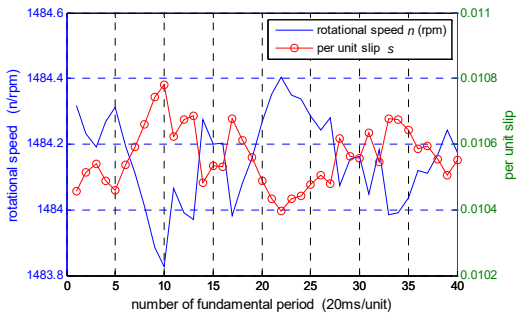

Fig. 3. Speed arithmetic means and slip of a motor.

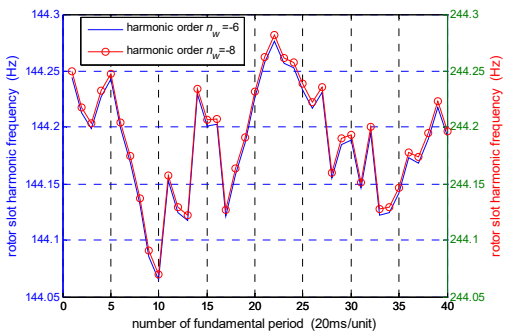

Fig. 4. Rotor slot harmonic under the conditions of $n_w = -6$ and $n_w = -8$.

Fig. 4 show the rotor slot harmonics under the conditions of $n_w = -6$ and $n_w = -8$. It is very important to predict a correct n_w since there are a total of $2 \times n_w$ repeated calculations which wastes a lot of the time of the RSH. The study of this issue has a great significance in terms of protection from the overheating faults of an inductance motor.

In order to select a suitable n_w, the stator voltage and current are sampled at up to 40kHz by a data acquisition card. The sampled stator current and its spectrum is shown in Fig. 5 and Fig. 6. As shown in Fig. 6, the sampling time was controlled in 0.8 second which consists of 40 fundamental periods.

As shown in Fig. 6, the left y-coordinate denotes the spectral amplitude which was obtained by a FFT (Fast Fourier Transform), and the right y-coordinate indicates the winding harmonic order n_w.

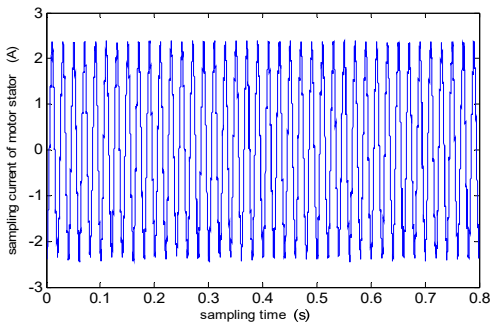

Fig. 5. Measured stator current of the motor.

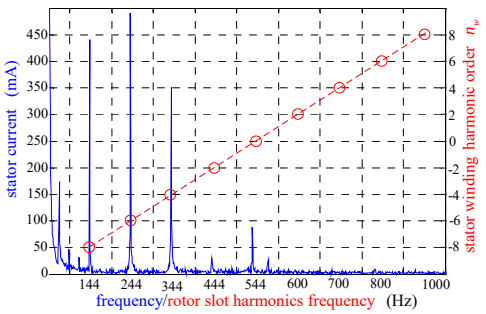

Fig. 6. Spectrum of the stator current.

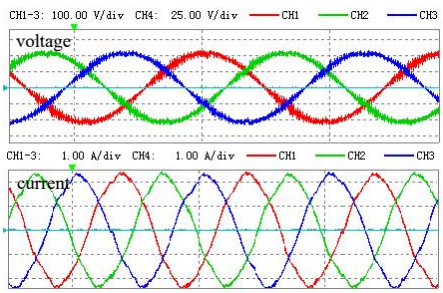

Fig. 7. Voltage and current of the power system.

Fig. 6 shows that due to the maximum amplitude of the stator current in 244Hz, $n_w^* = -6$ is selected as the winding harmonic order in actual engineering. The computation time of the present method is increased by about $2n_w$ times under the RSH.

There is a problem with the prediction order $n_w^* = -6$ and frequency $f_{sh}^* = 244\text{Hz}$ since it is very close to the frequency of the 5th harmonic current of the power supply. An important problems is making sure $f_{sh}^* = 244\text{Hz}$ is the slot harmonic frequency of the inductance motor or 5th harmonic current of the power system.

In an effort to solve this problem, the voltage and current of the power system are measured as shown in Fig. 7.

Moreover, Fig. 8 shows the measured spectrum of the stator current and the content of the harmonic current. It denotes that the amplitude of the 5th harmonic current is 0.015A, which is much less than the fundamental current 2.35A. There is not much doubt about that the harmonic

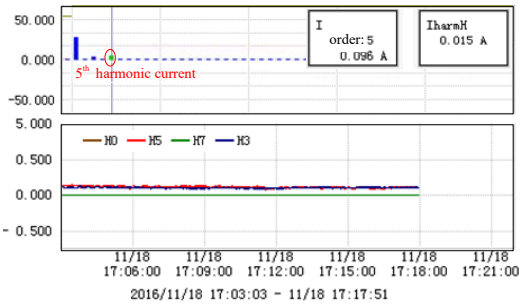

Fig. 8. Measured spectrum of the stator current.

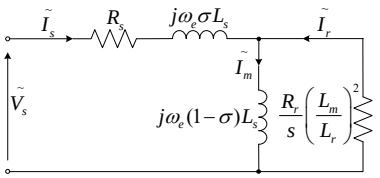

Fig. 9. Steady-state positive sequence motor equivalent circuit.

current with the frequency of 244Hz in Fig. 6 is generated by the rotor of the inductance motor.

Once the harmonic order n_w^* and frequency f_{sh}^* have been determined, the slip s can be expressed as follows:

$$s = 1 - 0.5p\left[f_{sh} / f_1 - n_\omega\right] / (kR) \tag{2}$$

This work provides an algorithm base to identify the rotational speed for an inductance motor based on pre-setting the harmonic order n_w^* and extracting the corresponding harmonic frequency f_{sh}^*. This can significantly improve the identification efficiency of the RSH, where the times of iterations have been significantly decreased.

III. Improvement of the RSH Accuracy

Considering that the load voltage sags and swells have an enormous influence on the identification accuracy of the motor parameters, which is the basis of estimating the motor temperature, attention is paid to overcoming the effects of the voltage flash and the current surge of the power supply in this chapter. For this purpose, the analysis expressions of the motor parameters such as the stator self-inductance have been derived based on modelling the inductance motor. Moreover, MPC has been used to forecast the parameters variation trend in order to suppress the effects of the voltage and current shocks that are caused by a power perturbation.

A. Analytical Expressions of the Motor Parameters

Based on the work done in [2], the steady-state positive sequence equivalent circuit of an inductance motor is shown in Fig. 9.

In Fig. 9, R_s and R_r are the stator resistance and rotor resistance, respectively; L_s, L_r and L_m are the stator leakage, rotor leakage and magnetizing inductance, respectively; $\tilde{V}_s$ and $\tilde{I}_s$ are the stator per-phase input voltage and current phasors, respectively; ω_e is the angular speed corresponding to the power supply frequency; σ is defined as $\sigma = 1 - L_m^{\ 2} / (L_r L_s)$; $\tilde{I}_r$ and $\tilde{I}_m$ are the rotor and magnetizing current, respectively.

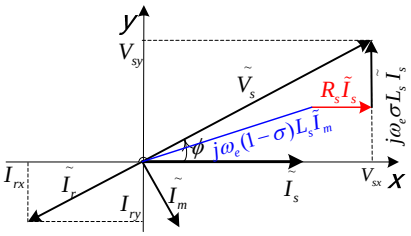

Fig. 10. Phasor diagram of the equivalent circuit.

As shown in Fig. 9, the steady-state motor operations can be described as follows

$$\tilde{V}_s = (R_s + j\omega_e L_s)\tilde{I}_s + j\omega_e(1-\sigma)L_s\tilde{I}_m \tag{3a}$$

$$0 = j\omega_e(1-\sigma)L_s\tilde{I}_s + [r_1 + j\omega_e(1-\sigma)L_s]\tilde{I}_r \tag{3b}$$

Where, the expression of r_1 is defined as $r_1 = R_r\left(L_m / L_r\right)^2 / s$.

In Fig. 10, defining V_{sx} and V_{sy} as the projection of $\tilde{V}_s$ onto the *x*-axis and *y*-axis, respectively, (3a) and (3b) can be expanded to a matrix form (4).

$$\begin{bmatrix} V_{sy} \\ V_{sx} \\ 0 \\ 0 \end{bmatrix} = \begin{bmatrix} \omega_e L_s & 0 & \omega_e(1-\sigma)L_s \\ R_s & -\omega_e(1-\sigma)L_s & 0 \\ \omega_e(1-\sigma)L_s & r_1 & \omega_e(1-\sigma)L_s \\ 0 & -\omega_e(1-\sigma)L_s & r_1 \end{bmatrix} \begin{bmatrix} I_s \\ I_{ry} \\ I_{rx} \end{bmatrix} \tag{4}$$

A compact matrix form (5) can be given by simplifying (4):

$$\begin{bmatrix} \omega_e I_s V_{sy} & -\omega_e^2 I_s^2 \end{bmatrix} \begin{bmatrix} (1+\sigma)L_s \\ \sigma L_s^2 \end{bmatrix} = V_s^2 + I_s^2 R_s^2 - 2R_s I_s V_{sx} \tag{5}$$

Then analytic solutions of the stator inductance L_s can be obtained by solving one variable quadratic equation for L_s based on mathematics mechanization theory [16]. This is one of the most important harvests in this paper based on [1] which uses a numerical iterative method to solve (4).

$$L_{s1} = 0.5\left(L_m^2\omega_e I_s + 2L_r V_{sy} + \beta\right) / \left(L_r\omega_e I_s\right) \tag{6a}$$

$$L_{s2} = 0.5\left(L_m^2\omega_e I_s + 2L_r V_{sy} - \beta\right) / \left(L_r\omega_e I_s\right) \tag{6b}$$

Where:

$$\beta = \sqrt{L_m^4\omega_e^2 I_s^2 + 4L_r^2 V_{sy}^2 - 4L_r^2 R_s^2 I_s^2 + 8L_r^2 R_s V_{sx} I_s - 4L_r^2 V_s^2}$$

, $V_{sx} = V_s\cos\phi$, $V_{sy} = V_s\sin\phi$, ϕ are the phase angle between the sampled voltage V_s and sampled current I_s.

Based on [2] an analytic expression of R_r has been derived as follows:

$$R_r = s\omega_e L_r\sqrt{\left[V_{sy} / I_s - \omega_e\left(L_s - L_m^2 / L_r\right)\right] / \left(\omega_e L_s - V_{sy} / I_s\right)} \tag{7}$$

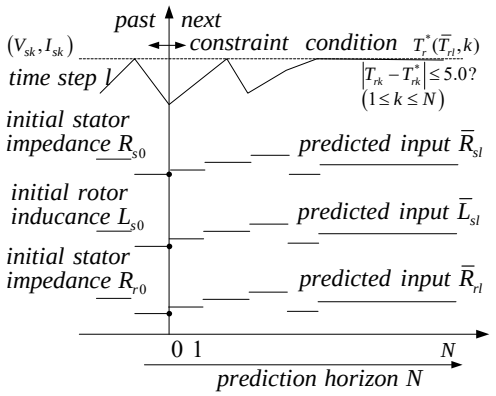

Fig. 11. Schematic diagram of MPC.

Since the parameters of the inductance motor are related to its temperature the intermediate variables $j\omega_e(1-\sigma)L_s I_m$ and $R_s I_s$ in Fig. 10 have been confirmed to be nonlinear.

At temperature T_{s0}, it is assumed that the stator resistance is R_{s0}, and that the corresponding stator temperature coefficient is α. The relationship between the stator temperature and the stator resistance R_s can be described as follows:

$$R_s = R_{s0} + (T_s - T_{s0})\alpha R_{s0} \tag{8}$$

As a supplementary, the relationship between the rotor temperature and the rotor resistance can be satisfied by the following expression:

$$T_r = [R_r / R_{r0}][T_{r0} + k_r] - k_r \tag{9}$$

Where, R_{r0} is the initial rotor resistance at the ambient temperature T_{r0}; R_r is the rotor resistance at the temperature T_r; and k_r is the temperature coefficient. It is common to think that $T_{r0} = T_{s0}$.

Considering that the parameters (R_s, L_s, R_r) are continuous variables associated with the temperature which are the inertia one, an approach should be explored to overcome the influence of the voltage shock and current surge on the identification accuracy of the above parameters.

B. Application of Model Predictive Control

MPC is an advance control technique that determines the motion phenomena by solving nonlinear equations online. The core idea is that at every sampling time l, the control state of the system x_k $(1 \le k \le N)$ can be forecasted. In this paper MPC is used to predict and correct the parameter perturbations caused by a sudden load change. This is intended to improve the identification accuracy of parameters such as R_s、L_s and R_r. This optimization is constrained by a specified minimal input sequence of the time horizon N, i.e. $x_k = (V_{sk}, I_{sk}) \in [(V_{s1}, \cdots, V_{sN}); (I_{s1}, \cdots, I_{sN})]$ $(k = 1, 2, \cdots N)$.

Then the optimization problem of the temperature identification would be solved at each time step l. The solution procedure of MPC is described as follows:

$$X_{sA}^*(\bar{R}_{sl}, k) = \min_{X_{s1}, \cdots X_{sN}} \sum_{k=1}^{N} \left\| X_{sk} - \bar{X}_{sl} \right\|_R^2 \quad (X = R, L) \tag{10}$$

$$R_{rA}^*(\bar{R}_{rl}, k) = \min_{R_{r1}, \cdots R_{rN}} \sum_{k=1}^{N} \left\| R_{rk} - \bar{R}_{rl} \right\|_R^2 \tag{11}$$

$$for \ \ any \ \ (V_{sk}, I_{sk}), \ \ |T_{rk} - T_{rk}^*| \le 5.0 \ \ ? \tag{12}$$

$$\begin{aligned} s.t. \ \ & \bar{R}_{sl} = R_{sk} \quad \bar{L}_{sl} = L_{sk} \quad \bar{R}_{rl} = R_{rk} \\ & \bar{T}_{rl} = f(\bar{R}_{sl}, \bar{L}_{sl}, \bar{R}_{rl}) \end{aligned} \tag{13}$$

$$\begin{aligned} & x_k = \sqrt{\left(\sum_{k=N_{\min}=1}^{N\max} X_{sk}^2 \right) / N} \quad (x = u, i; X = V, I) \\ & for \ \ any \ \ (V_{sk}, I_{sk}), \ \ if \ \ |u_{k+1} - u_0| \ge 15 \ \ and \\ & |u_k - u_{k-1}| \ge 15.0 \ \ and \ \ |u_k - u_{k+1}| \ge 15.0 \\ & do \ \ u_k = 0.5(u_{k-1} + u_{k+1}) \end{aligned} \tag{14}$$

Where, $(R_{s1}, \cdots, R_{sN})$, $(L_{s1}, \cdots, L_{sN})$ and $(R_{r1}, \cdots, R_{rN})$ are optimization variables, $(\bar{R}_{sl}, \bar{L}_{sl}, \bar{R}_{rl})$ is the steady state at the time l, and $\bar{T}_{rl} = f(\bar{R}_{sl}, \bar{L}_{sl}, \bar{R}_{rl})$ indicates the system temperature at the time step l. The rotor temperature T_r can be derived by substituting (R_{s0}, L_{s0}, R_{r0}) into (9).

A flowchart of MPC can be illustrated by Fig.11. At each time step l, the state (V_{sk}, I_{sk}) $(k = 1, 2, \cdots N)$ of the system is measured. Then the optimal input $(\bar{R}_{sl}, \bar{L}_{sl}, \bar{R}_{rl})$ is computed so that the objective function T_{rk} is optimized.

The optimization rule of MPC is to obtain the minimum identification error of the temperature T_r by predicting the corresponding steady parameters $(\bar{R}_{sl}, \bar{L}_{sl}, \bar{R}_{rl})$ at every time step l within the optimization horizon $N_{\max}$. Based on MPC, the (10) to (11) can be rewritten as follows:

$$X_{sB}^*(\bar{X}_{sl}, k) = \min_{k \in \mathbb{N}} R_{sk} \quad (X = R, L) \tag{15}$$

$$R_{rB}^*(\bar{R}_{rl}, k) = \min_{k \in \mathbb{N}} R_{rk} \tag{16}$$

$$k \in \mathbb{N} = [N_{\min}, N_{\max}], \ \ l = N_{\max} - N_{\min} \tag{17}$$

The relationship between the variables l, $N_{\min}$ and $N_{\max}$ is illustrated in Fig. 12. Where, N is the real time; $N_{\max}$ is the maximum optimization horizon; $N_{\min}$ is a minimum bound, which makes it possible to reduce the sensitiveness with respect to measurement noise; l is the sampling time, where the up limit and down limit are $N_{\max}$ and $N_{\min}$, respectively. An input sequence which contains $(N_{\max} - N_{\min})$ sampling data is obtained within the sampling time l. For the sampling

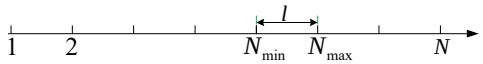

Fig. 12. relationship between the variables l , $N_{\min}$ and $N_{\max}$.

TABLE I
PROCEDURE OF THE MOTOR PARAMETER PREDICTION BY MPC

0	Initial values: $R_{s0}, R_{r0}, L_r \;\; n_w = -6$, $k = 1$, $u_0 = 220\text{V}$
1	(I_{sk}, V_{sk}) (first sampling period) positive sequence analysis of the voltage and current calculate power factor angle ϕ $V_{skx} = V_{sk}\cos\phi$, $V_{sky} = V_{sk}\sin\phi$
2.1	$L_{sk} = f(R_{sk}) = 0.5\left(L_m^2\omega_e I_{sk} + 2L_{rk}V_{syk} + \beta\right)/\left(L_{rk}\omega_e I_{sk}\right)$
2.2	$R_{rk} = s\omega_e L_r\sqrt{\left[V_{sy}/I_s - \omega_e\left(L_s - L_m^2/L_r\right)\right]/\left(\omega_e L_s - V_{sy}/I_s\right)}$
2.3	$R_{sk} = R_{s0} + \left(T_{sk} - T_{s0}\right)\alpha R_{s0}$
3.1	$T_{rk} = \left(R_{rk}/R_{r0}\right)\left(T_{r0} + k_r\right) - k_r$
3.2	If $\left\|T_{rk} - T_{rk}^*\right\| \le 5$ $\left(T_{rk}^*$ denotes measured temperature$\right)$
3.3	then $\bar{R}_{sl} = R_{sk}$; $\bar{L}_{sl} = L_{sk}$; and $\bar{R}_{rl} = R_{rk}$; $\bar{T}_{rl} = T_{rk}$ (output temperature of the k^{th} fundamental period);
4	end

voltage and the current of the motor stator $l = 20\text{ms}$ is selected.

Supposing T_r and T_r^* denote the identification temperature and the measured temperature of the motor at the time step k , then T_r can be illustrated as follows:

$$T_{rB}^*(\bar{T}_{rl}, k) = \begin{cases} T_{rk} \;\; if \;\; \left|T_{rk} - T_{rk}^*\right| \le 5.0 \\ else \;\; call \;\; Eq.(14) \;\; calculate \;\; T_{rk} \;\; again \end{cases} \quad (18)$$

The ability of MPC to predict and correct the motor parameters is of benefit for improving the identification accuracy of the rotor temperature by overcoming its hysteresis. The application procedure of MPC is shown in Table I.

IV. EXPERIMENT RESULTS

In order to validate the feasibility and effectiveness of the proposed approach, an experimental platform has been designed in this paper. This platform is used to demonstrate the online performance of the proposed identification method to reduce the negative effect of power voltage shocks. As shown in Fig. 13 and Table II, a 1.5kW AC motor without any cooling fan, which is the same as the motor mentioned in section II has been considered.

The signal modulating circuit is designed to provide the sampling voltage and sampling current to the data acquisition card PCI-1711, where the sampling frequencies are 40 kHz.

Fig. 14 shows the measured stator temperature obtained from the temperature test device TMP-A for 30 minutes.

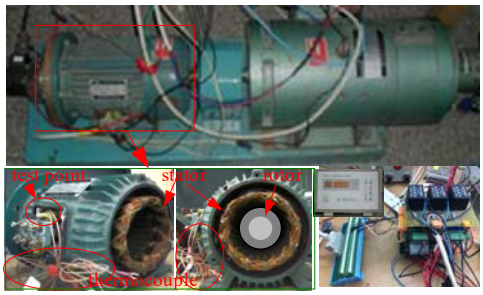

Fig. 13. Schematic diagram of the experimental device.

TABLE II.
THE PARAMETERS OF A MOTOR UNDER THE CONDITION OF $T_{s0} = T_{r0} = 18^\circ\text{C}$

Parameters	Symbols	Values
stator resistance	R_s	3.800Ω
rotor resistance	R_r	0.365Ω
stator self-inductance	L_s	2.000mH
rotor self-inductance	L_r	2.000mH
mutual inductance	L_m	0.700mH
rated voltage	$\tilde{V}_s$	220V
rated current	$\tilde{I}_s$	3.700A
rated speed	n	1500r/min
rated power	$\tilde{I}_s$	1.900kw
pole number	p	4
power supply frequency	f	50Hz
dominant rotor slot number	R	22
temperature coefficient	k_r	225
stator temperature coefficient	α_s	0.01/ºC
winding distribution harmonic order	n_w	-6

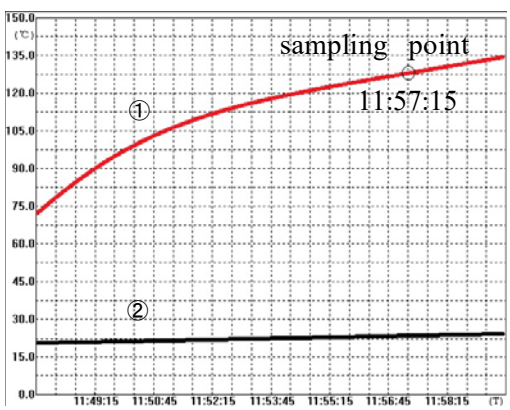

Fig. 14. Measured temperature of the stator.

Where curve ① is the measured stator temperature, and curve ② is the measured ambient temperature.

The temperature is gradually increased from a temperature of 74°C which is obtained after the motor ran for 1 hour. At the time of 11:57:15 the data acquisition card is used to sample the stator voltage and current for 0.8s. Then 32000 data are obtained, which consist of 40 fundamental periods. Then a measured sequence of the voltage and current

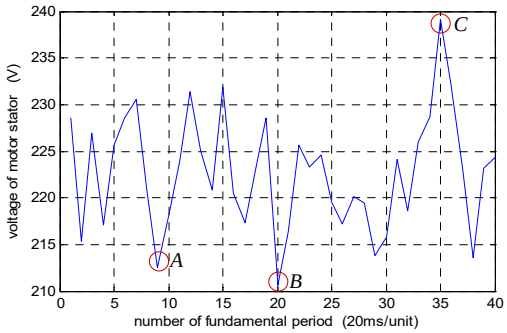

Fig. 15. Measured stator voltage of the motor.

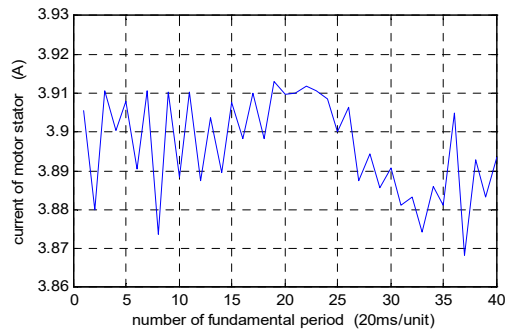

Fig. 16. Measured stator current of the motor.

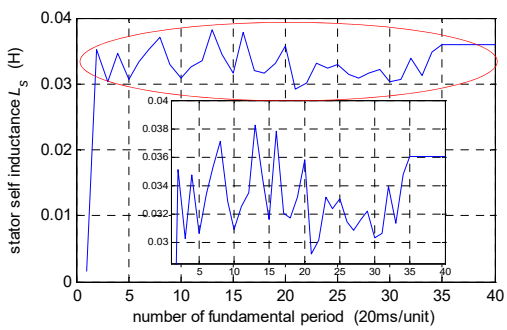

Fig. 17. Predictive value of the stator inductance.

$\{40\times 2,\ [(V_{s1},\cdots,V_{rN});(I_{s1},\cdots,I_{rN})]\}$ can be obtained which are shown in Fig. 15 and Fig. 16, where $N=40$, $N_{\min}=1$, and $N_{\max}=800$.

Fig. 15 and Fig. 16 show the sampling voltage and sampling current, respectively. Fig. 15 indicates that there are significant changes in the sampling voltage such as A, B and C which influence the identification accuracy of the rotor temperature.

As shown in Fig. 17 the inductance L_s can be obtained from (6a) by substituting $(n_w=-6, f_{sh}=244)$ into (2) based on Table II. This indicates that there are the similar shocks of the stator inductance in Fig. 15.

In fact, the inductance grew from the originally 2.0mH to approximately 35mH which has a huge influence on further estimation of the rotor temperature.

Similar to the process used before, Fig. 18 shows the rotor resistance R_r obtained from (7), which also has significant

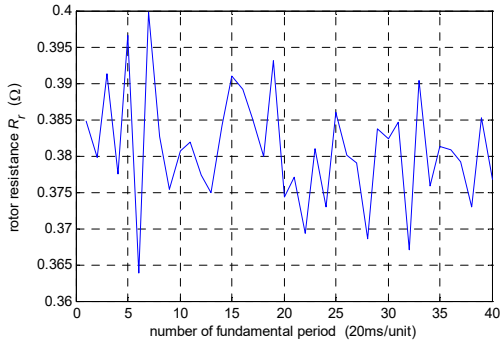

Fig. 18. Predictive value of the rotor resistance.

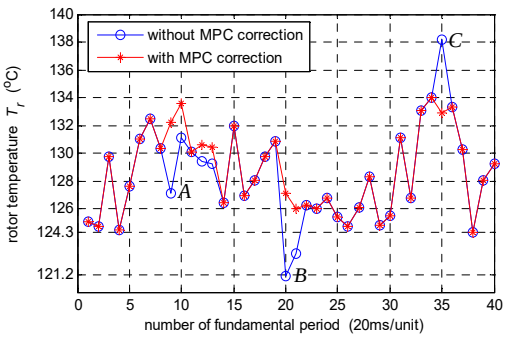

Fig. 19. Estimated rotor temperature of the motor.

changes due to voltage shocks. This denotes that the rotor resistance varies between 0.365 Ω and 0.400 Ω. The perturbation of the rotor impedance can also affect the identification accuracy. On the other hand, due to (7), the varied process of inductance L_s has been illustrated rapidly and effectively.

The above analysis shows that there is an intense volatility of the motor parameters due to the terrible discontinuities of the stator voltage and current. In order to improve the identification accuracy of the rotor temperature, the perturbations of the motor parameters, such as $(\bar{R}_{sl}, \bar{L}_{sl}, \bar{R}_{rl})$, which are caused by sags or swells of the stator voltage and current, should be corrected.

The correcting results using MPC are shown in Fig. 19. Where ⊖ represents the results without MPC correction and ✳ represents the results with MPC correction. It is easy to see the advantage of MPC for correcting the identification error by revising the motor parameters at stator voltage shocks.

The A, B, and C points in Fig. 19 correspond to those in Fig. 15 based on Table I. It is shown that the relative error of the temperature is obviously smaller than that without MPC.

It is assumed the stator temperature is approximately 1°C lower than the rotor temperature. As shown in Fig. 14, the measured stator temperature of curve ① at time 11:57:15 is 128°C. Therefore, the corresponding measured rotor temperature is $T_r^* \approx 128+1=129$°C. This shows that the temperature perturbation has been corrected based on the

TABLE III
ERROR OF THE PROPOSED APPROACH TO THE MEASURED TEMPERATURE

Data	Without MPC		With MPC	
Term	Value	Error	Value	Error
maximum	138.00	**9.00**	134.00	**5.00**
minimum	121.20	**7.80**	124.30	**4.70**
average	129.60	**0.60**	129.15	**0.15**

procedure of Table I due to the MPC. The error of the estimating rotor temperature when compared with the measuring temperature $\left|T_r^* - T_r\right|$ is shown in Table III.

As shown in TABLE III, it is easy to see that the error is significantly reduced by using MPC. The maximum error is reduced from $9^\circ\mathrm{C}$ to no more than $5^\circ\mathrm{C}$ and the average error is only $0.15^\circ\mathrm{C}$.

V. CONCLUSIONS

An approach that can be used to improve both the calculation efficiency and identification accuracy of the RSH is proposed. One of the aims of this study is to predict the stator winding distribution harmonic order based on the current spectrum analysis. The other aim is using MPC to correct the perturbation of the identification parameters of the motor caused by voltage shocks and current surges of power systems. An online estimation procedure for achieving the above objectives is proposed based on derived expressions of the parameters of an inductance motor. All of the above methods have been validated by extensive experimental results.

Temperature monitoring of rotor winding is an urgent need of inductance motors such as electric submersible motors and wind power generators. If a useful method is not used, it may not be possible to effetely protect these motors, and some undesirable result may arise unexpectedly. As a result, this paper focuses on improving the efficiency and accuracy of the RSH by MPC based on estimating the harmonic order, and suppressing the parameters distortion of the inductance motor. Experimental results show that this work can be used as a reference for highly efficient and reliable protection of inductance motors from overheating in actual engineering.

REFERENCES

[1] Z. Gao, T. G. Habetler, R. G. Harley, and R. S. Colby, "A sensorless rotor temperature estimator for induction machines based on a current harmonic spectral estimation scheme," *IEEE Trans. Ind. Electron*., Vol. 55, No. 1, pp. 407-416, Jan. 2008.

[2] Z. Gao R. S. Colby, L. Turner, and B. Leprettre, "Filter design for estimating parameters of inductance motor s with time-varying loads," *IEEE Trans. Ind. Electron.*, Vol. 58, No. 5, pp. 1518-1529, Jun. 2010.

[3] A. G. Yepes, F. Baneira, J. Malvar, A. Vidal, D. Pérez-Estévez, O. López, and J. Doval-Gandoy, "Selection criteria of multiphase induction machines for speed-sensorless drives based on rotor slot harmonics," *IEEE Trans. Ind. Electron*., Vol. 63, No. 8, pp. 4663-4673, Mar. 2016.

[4] S. Williamson and Y. N. Feng, "Slot-harmonic fields in closed-slot machines," *IEEE Trans. Ind. Application,* Vol. 44, No. 4, pp. 1165-1171, Jul. 2008.

[5] Y. Xu, J. Zhao, and X. Fu, "Quantitative analysis for influence of structure parameters on the slot harmonic in fractional-slot permanent magnet motors," in *Proc. ICEMS*, pp. 349-353, 2014.

[6] Seungdeog Choi, B, Akin, M, M. Rahimian, and H. A. Toliyat, "Performance-oriented electric motors diagnostics in modern energy conversion systems," *IEEE Trans. Ind. Electron.* , Vol. 59, No. 2, pp.1266-1277, Feb. 2012.

[7] C. M. Apostoaia, "Multi-domain system models integration for faults detection in induction motor drives," in *Proc. ICE/IT*, pp. 388-393, Aug. 2014.

[8] M. Smochek, A. F. Pollice, M. Rastogi, and M. Harshman, "Long cable applications from a medium-voltage drives perspective," *IEEE Trans.* Magn., Vol. 52, No. 1, pp. 645-652, Jan. 2016.

[9] Hassan Farhan Rashag, S. P. Koh, A. N. Abdalla, N. M. L. Tan, and K. H. Chong, "Modified direct torque control using algorithm control of stator flux estimation and space vector modulation based on fuzzy logic control for achieving high performance from induction motors," *Journal of Power Electronics*, Vol. 13, No. 3, pp. 369-379, May 2013.

[10] Z. Yin, G. Li, C. Du, X. Sun, J. Liu, and Y. Zhong, "An adaptive speed estimation method based on a strong tracking extended Kalman filter with a least-square algorithm for induction motors," *Journal of Power Electronics*, Vol. 17, No. 1, pp. 149-160, May 2013.

[11] N.-S. Park, M.-H. Jang, J.-S. Lee, K.-S. Hong, and J.-M. Kim, "Performance improvement of a PMSM sensorless control algorithm using a stator resistance error compensator in the low speed region," *Journal of Power Electronics*, Vol. 10, No. 5, pp. 485-490, Sep. 2010.

[12] L. Van den Broeck, M. Diehl, and J. Swevers. "A model predictive control approach for time optimal point-to-point motion control," *Mechatronics*, Vol. 21, pp. 1203-1212, Jul. 2011.

[13] M. Vatani, B. Bahrani, M. Saeedifard, and M. Hovd, "Indirect finite control set model predictive control of modular multilevel converters," *IEEE Trans. Smart Grid*, Vol. 6, No. 3, pp. 1520-1529, May 2015.

[14] M. Preindl and S. Bolognani, "Model predictive direct speed control with finite control set of PMSM drive systems," *IEEE Trans. Power Electron.*, Vol. 28, No. 2, pp. 1007-1015, Jun. 2012.

[15] F. Wang, S. A. Davari, Z. Chen, Z. Zhang, D. A. Khaburi, J. Rodríguez, and R. Kennel, "Finite control set model predictive torque control of induction machine with a robust adaptive observer," *IEEE Trans. Power Electron.*, Vol. 64, No. 4, pp. 2631-2641, Feb. 2016.

[16] L. Wang, X. Zhang, D. Xu, and W. Huang, "Study of differential control method for solving chaotic solutions of nonlinear dynamic system," *Nonlinear Dynamics*, Vol. 67, No. 4, pp. 2821-2833, Sep. 2011.

Liguo Wang was born in Heilongjiang Province, China, in 1972. He received his B.S. degree from the Harbin University of Science and Technology, Harbin, China, in 1994; and his M.S. and Ph.D. degrees in Electrical Engineering from the Harbin Institute of Technology, Harbin, China, in 1999 and 2002, respectively. Since 2003, he has been with the Department of Electrical and Electronics Engineering, Harbin Institute of Technology, where he is presently working as a Professor. From 2015 to 2016, he was a Visiting Scholar at Cornell University, Ithaca, NY, USA. His current research interests include nonlinear control theory, sensorless motor control, and smart grids.

Qingyue Jiang was born in Jiangsu Province, China, in 1993. She received her B.S. degree from the Harbin Institute of Technology, Harbin, China, in 2015, where she is presently working towards her M.S. degree in the School of Electrical Engineering and Automation. Her current research interests include on-line parameter identification of induction motors and model predictive control.

Chaoyu Zhang was born in Jilin Province, China, in 1992. He received his B.S. degree from the East China Jiaotong University, Nanchang, China, in 2014. He is presently working towards his M.S. degree in the School of Electrical Engineering and Automation, Harbin Institute of Technology, Harbin, China. His current research interests include parameter identification in ac motors.

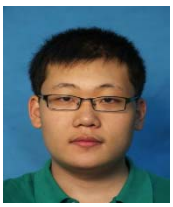

Dongxin Jin was born in Heilongjiang Province, China, in 1993. He received his B.S. degree from the Harbin Institute of Technology, Harbin, China, in 2016, where he is presently working towards his M.S. degree in the School of Electrical Engineering and Automation. His current research interests include model predictive control and smart grid control.

Hui Deng was born in Heilongjiang Province, China, in 1966. He received his B.S. degree from the Harbin Institute of Technology, Harbin, China, in 1989; his M.S. degree from the Harbin Engineering University, Harbin, China, in 1998; and his Ph.D. degree in Electrical Engineering from the Harbin Institute of Technology, in 2008. Since 1989, he has been with the Daqing Oilfield Powerlift Pump Industry Co. Ltd, Daqing, China, where he is presently working as a General Engineer. From 2003 to 2004, he was a Visiting Scholar at the University of Waterloo, Waterloo, ON, Canada. His current research interests include sensorless parameters identification and motor design.